An experimental study on the effects of friction modifiers on wheel–rail dynamic interactions with various angles of attack

Yang, Zhen; Zhang, Pan; Moraal, Jan; Li, Zili

An experimental study on the effects of friction modifiers on wheel–rail dynamic interactions with various angles of attack

Zhen Yang[1] · Pan Zhang[1] · Jan Moraal[1] · Zili Li[1]

Abstract By modifying friction to the desired level, the application of friction modifiers (FMs) has been considered as a promising emerging tool in the railway engineering for increasing braking/traction force in poor adhesion conditions and mitigating wheel/rail interface deterioration, energy consumption, vibration and noise. Understanding the effectiveness of FMs in wheel–rail dynamic interactions is crucial to their proper applications in practice, which has, however, not been well explained. This study experimentally investigates the effects of two types of top-of-rail FM, i.e. FM-A and FM-B, and their application dosages on wheel–rail dynamic interactions with a range of angles of attack (AoAs) using an innovative well-controlled V-track test rig. The tested FMs have been used to provide intermediate friction for wear and noise reduction. The effectiveness of the FMs is assessed in terms of the wheel–rail adhesion characteristics and friction rolling induced axle box acceleration (ABA). This study provides the following new insights into the study of FM: the applications of the tested FMs can both reduce the wheel–rail adhesion level and change the negative friction characteristic to positive; stick–slip can be generated in the V-Track and eliminated by FM-A but intensified by FM-B, depending on the dosage of the FMs applied; the negative friction characteristic is not a must for stick–slip; the increase in ABA with AoA is insignificant until stick–slip occurs and the ABA can thus be influenced by the applications of FM.

1 Introduction

Wheel–rail friction management is a challenge for railway operators and infrastructure managers. A minimum level of friction must be guaranteed to ensure appropriate braking and traction of trains, whereas high friction increases wear and rolling contact fatigue of wheels and rails, energy consumptions and noise emissions. By modifying friction to the desired level, applications of friction modifiers (FMs) have been considered as an emerging tool for effectively increasing the braking or traction forces in poor adhesion conditions [1, 2], and mitigating wheel/rail interface deterioration [3], energy consumption [4], friction-induced squeal noise and short pitch corrugation [5–7].

The railway operators and infrastructure managers mostly rely on practical observations that do not elucidate completely the effectiveness of the FM used on their network [2]. A better understanding of the effectiveness of FMs in wheel–rail dynamic interactions, i.e. frictional contact accompanied by structural vibration [8], is highly desired for their proper applications in practice. The effectiveness of FMs in railway practice depends mainly on wheel–rail creepage [1] and the dosage of the product that is applied [3, 9].

The effects of FMs on wheel–rail contact with the longitudinal creepage have been widely studied with laboratory [1] and field [10] tests, because the adhesion in the longitudinal direction is a subject of vital interest for traction/braking [11], affecting safety and punctuality of railway transportation. FMs can also advance wheel–rail contact behaviour

✉ Zili Li
  z.li@tudelft.nl

[1] Section of Railway Engineering, Delft University of Technology, Stevinweg 1, 2628 CN Delft, The Netherlands

when the lateral creepage is significant. Efforts have been taken to practically improve bogie performance [12] and reduce squeal noise and corrugation at curves [5–7, 13, 14] with the applications of FMs. However, the effectiveness of FMs has not been well explained for wheel–rail contact with different lateral creepage due to the low level of control of operating parameters in the field, such as angle of attack (AoA) [14].

The optimal dosage, or application rate, of FMs varies case by case. It depends greatly on the FM type [9] and wheel–rail contact condition, e.g. interface contamination [15] and adhesion level [16]. Optimisation has been achieved for the reduction of specific types of problems [3, 7, 12]; however, there seems to be a lack of study on the FM dosage and its influence on wheel–rail adhesion characteristics under well-controlled conditions.

Furthermore, although noise emission has been addressed in the studies of FM, the effect of FM on wheel–rail friction-induced vibration, as the source of noise, has rarely been reported. That is probably because in field tests, noise can be more handily measured, e.g. no need to access the track, than the wheel/rail structural vibration; and in the laboratory, most of the broadly used test rigs such as the twin-disc roller rig fail to simulate realistic wheel–rail dynamic interactions because of the absence of key track/train components [17, 18]. Further exploration into the effect of FM on the friction-induced vibration is thus desirable for the mitigation of squeal, corrugation and wheel polygonisation [19].

To improve the understanding of the effectiveness of FMs in railway practice, this study experimentally investigates the effects of two types of FM, denoted as FM-A and FM-B, on wheel–rail dynamic interactions with different lateral creepage. The water-based FM-A and oil-based FM-B are widely used in the Dutch and Belgian railways, respectively. FM-A is a type of top-of-rail FM, and FM-B can be used as a top-of-rail as well as flange lubricant. Both of them are on-board FMs that can be sprayed by the in-service trains. The tests were conducted in V-Track [17], an innovative test rig that can simulate realistic wheel–rail dynamic interactions and

accurately control and measure wheel–rail normal load, friction force and creepage in the longitudinal and lateral directions [20]. Different dosages of the FMs were applied along the ring rail of V-Track. The effectiveness of the FMs was assessed by analysing the wheel–rail adhesion characteristics and frictional rolling induced axle box acceleration (ABA) under the dry and FM-treated conditions with various AoAs. This study provides insights into the proper applications of FM in railway tracks.

2 Methodology

2.1 V-track test rig

Because the wheel–rail friction level and contact behaviour may vary with contact pressure, rolling speed, environmental temperature and humidity conditions, these factors need to be kept constant or controlled in the study of the effectiveness of FMs. The V-track test rig reproduces wheel–rail frictional rolling contact under well-controlled reproducible laboratory conditions. It consists of a maximum of four-wheel assemblies running over a ring rail system with a radius of 2 m, as shown in Fig. 1a. The ring rail system is composed of four pieces of rails with the standard S7 profile connected by joints. Due to the difficulty in manufacturing the circled rails, the ring rail is not perfectly circular but slightly elliptical. The wheel–rail contact behaviour may thus be different between two adjacent rails but quite similar on every two opposite rails. Supported by railpads, the rails are fixed on 100 evenly distributed steel sleepers by fasteners. Rubber pads are laid underneath the sleepers to simulate the stiffness and damping of a ballast layer. In the configuration of the current work, one wheel assembly is used to obtain the best control of the wheel–rail contact force and creepage. As shown in Fig. 1b, the wheel assembly is mounted on an arm of a steel frame vertically loaded through two springs. The scaled wheel has a diameter of 130 mm. A motor drives the steel frame so that the wheel assemblies
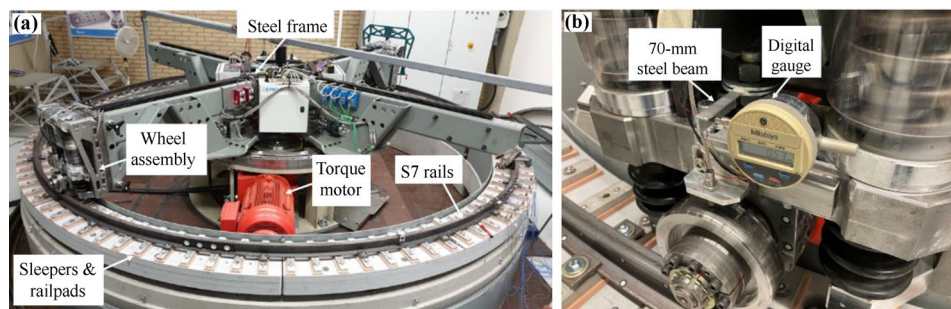

Fig. 1 The structure of V-track: **a** overview of V-track; **b** a digital gauge for the AoA measurement

can be pulled to move along the ring rail with a speed up to 40 km/h. Another motor is connected to the wheel through a braking shaft, which can apply appropriate negative/positive torque to generate braking/traction forces. The wheel AoA, adjustable between $-2°$ and $+2°$, is measured by a digital gauge mounted on the guiding block, which indicates the distance to a steel beam that rotates together with the axle box. The steel beam has a length of 70 mm which means that 1 mm equals a 0.8° rotation of the wheel axle. The estimated error in the AoA measurement is approximately 6% for a range of $\pm 0.5°$. The wheel–rail contact force can be reliably measured in three directions with a force measurement system called dynamometer [20]. The sampling frequency of the dynamometer is 16.67 kHz. Three 1D accelerometers are mounted on the wheel axle box to measure the ABA in the vertical, longitudinal and lateral directions. The sampling frequency of the ABA measurement is 100 kHz. A more detailed description of the V-Track structure and components can be found in [17, 20].

2.2 Test procedure

The tests with the applications of FM-A and FM-B were conducted on 4 and 17 February 2021, respectively. The ambient temperature was around 20 °C, and the relative humidity ranged between 36 and 37.1% and between 39 and 39.5% on the two testing days, respectively. The wheel–rail interface was carefully cleaned with acetone and dried with a hot-air blower (see Fig. 2) after the test using FM-A to guarantee the wheel–rail friction went back to the level of the original dry clean condition before the FM-B test and thus the testing results of FM-A and FM-B are comparable.

On each testing day, V-track was first run with a nominally zero AoA at a speed of 4 km/h under a dry, clean wheel–rail contact condition. The nominal wheel load was 4500 N, producing a Hertzian contact pressure of

Fig. 2 The rails were cleaned and dried with a hot-air blower between the tests with FM-A and FM-B

approximately 1.2 GPa [20], which is representative of the contact between the wheel tread and rail head for passenger trains in the Netherlands. The testing data including the wheel–rail contact force and ABA in three directions were automatically recorded during the test runs. The AoA was then increased progressively with a step of 0.08°. A gradual increase in the lateral wheel–rail contact force was observed until the friction was saturated. The friction saturation under the dry clean wheel–rail contact condition can be identified by the stick–slip oscillation, i.e. gradual increases of the time history curve followed by sudden drops (see an example later in Fig. 4), of the measured lateral contact force as well as the adhesion coefficient. The test procedure was then repeated under the FM-treated conditions.

Different dosages of FM were tested sequentially by applying 1/4, 1/2 and 1 droplet of the FMs along the 12.56-m ring rail. The FM dosage used in the Dutch railway ranges between 3.5 and 7 mm³ per rail metre. Since the wheel–rail contact patch in the V-track is 1/10 of that in the field practice, the dosage applied to the V-track may range between 0.35 and 0.7 mm³ per rail metre. The 1/4 droplet cases applied 0.6 mm³/m FMs to the V-track, corresponding well to the actual application. With a standard syringe, 1 droplet of both FMs weights 0.045 g ($\pm$0.002 g), as shown in Fig. 3a for FM-A. The 1-droplet dosage thus corresponds to an application rate of 3.6 mg per metre of the downscaled V-Track rail. Currently, the practice of how best to deliver the FM is often based on experience [9]. In this study, with a small screwdriver, the FMs of the testing dosage were divided into very small portions and applied to the rail top (see Fig. 3b). There are in total 25 small droplets of FM and thus application points over the rail circle. The portions manually applied along the rail could be unequal, but as they were spread out (squeezed to a steady-state layer) by the running wheel, the FMs would be evenly distributed by running V-track for 50 cycles at a speed of 10 km/h, as shown in Fig. 3c. The FMs can be sufficiently mixed with oxides in this process. Note that the FMs were applied on the rails prior to the test runs, not continuously supplied during the tests.

In total, eight cases were thus tested on the two testing days, as listed in Table 1. Tests 1–8 refer to the tests under the original dry clean condition, with the applications of 1/4, 1/2 and 1 droplet of FM-A, dry clean test before using FM-B, tests with 1/4, 1/2 and 1 droplet of FM-B, respectively. The influences of AoA and FM dosage on wheel–rail adhesion characteristics and ABA were then analysed to assess the effectiveness of the FMs.

2.3 Test data processing

The wheel–rail adhesion characteristics can be characterised by the adhesion coefficient (AC), i.e. the ratio between the magnitudes of wheel–rail friction force (the resultant
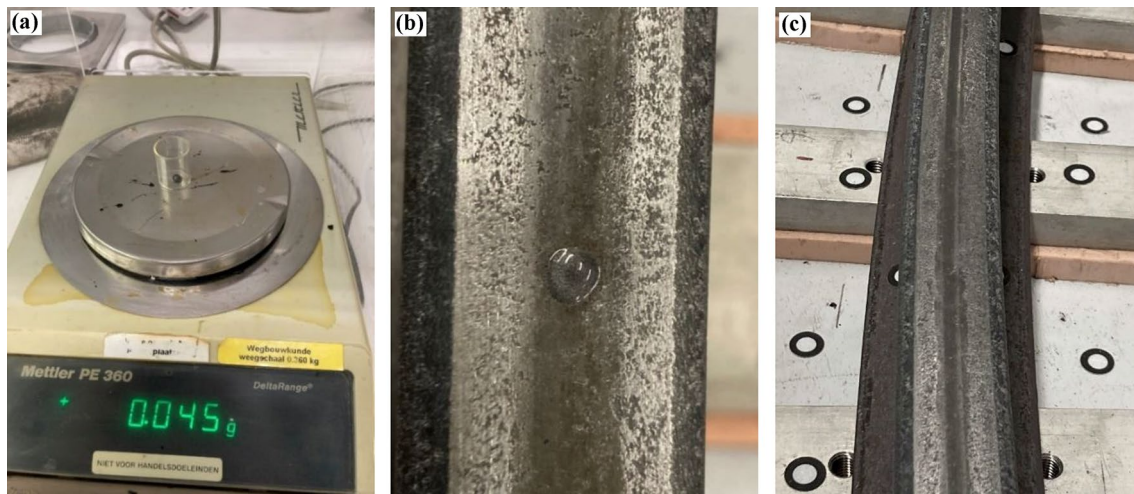
Fig. 3 The application of FM-A to V-track: **a** the read-out of 1 droplet of FM; **b** a small portion applied to the rail; **c** FM distributed on the running band

Table 1 Testing cases

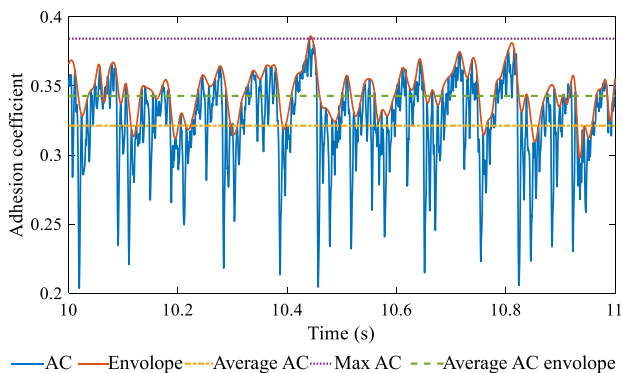| Dosage of the FMs	FM-A tests on 4 Feb	FM-B tests on 17 Feb
0 droplet: dry and clean rail	Test 1	Test 5
1/4 droplet	Test 2	Test 6
1/2 droplet	Test 3	Test 7
1 droplet	Test 4	Test 8

Fig. 4 Average vs maximum vs average of the upper envelope of the measured AC

of the lateral and longitudinal forces) and normal load. The measured AC varies with wheel–rail contact force over time during the wheel–rail friction rolling. An example of the AC time history measured under the original dry condition (test 1) with AoA = 0.48° is presented in Fig. 4, which shows typical stick–slip oscillation.

To determine the coefficient of friction (COF), i.e. the upper bound of AC, and to map out the creep curve, i.e. AC given as a function of creepage, a representative value of AC needs to be selected from the measured AC at each creepage level. Because the measured AC may vary greatly due to the occurrence of stick–slip (shown as the gradual increases followed by sudden drops of the measured AC time history) as shown in Fig. 4 or due to the uncertainties in contact condition and loading [21], the selection of the representative AC is critical and sometimes results in conflicting conclusions [22]. The maximum [23] and average [24–26] values of the measured AC are generally used as the representatives. However, it has been found that the maximum value may take place randomly due to the uncertainties in surface topography, hardness and cleanliness [25] as well as the variation of creepage during wheel rolling, sometimes causing peculiar trends of the results [22], while the average values are likely to underestimate the level of adhesion, especially when stick–slip occurs [21]. To overcome these problems and considering that COF is the upper bound of AC, this study proposed a new approach to determine the representative AC at each AoA (or creepage) level: the average of the upper envelope of the measured AC time history is considered as the adhesion level at the corresponding AoA. The envelope was calculated using spline interpolation over local maxima of AC time history separated by 100 samples. A comparison of the maximum value, average value and the average of the upper envelope of the measured AC time history is demonstrated in Fig. 4. We can see that the adhesion level determined by this new approach is between those determined by the maximum and average of the measured AC.

3 Results

3.1 Influence of AoA

3.1.1 Influence on wheel–rail adhesion under dry and FM-treated conditions

The influence of AoA on wheel–rail adhesion characteristics and ABA was investigated under the dry and FM-treated contact conditions. Figure 5 shows the measured time histories of ACs over the V-track circle with the increasing AoA with a step of 0.08° in the original dry condition (test 1). In each V-track test cycle, the testing data starts to be recorded when the wheel is rolling on rail 4 (R4). Then, the wheel sequentially passes rail 1 (R1), rail 2 (R2) and rail 3 (R3). The time histories of AC measured in one V-Track test cycle, shown in Fig. 5a and some other figures of this paper, are divided by black vertical lines to separate the

results measured on the four rails, denoted as 'R1', 'R2', 'R3' and 'R4'. The sharp peaks of the ACs at the black lines are caused by wheel–rail impacts at the four rail joints.

We can see from Fig. 5 that the measured AC increases with AoA as expected. When the friction saturation is achieved, stick–slip occurs on all the four rails: the AC increases to the amplitude until slip occurs, shown as a precipitous drop, and then, the contact returns to the stick state until the next slip is reached. The stick–slip can be more obviously seen from the close-ups of the AC time histories measured on each rail plotted in Fig. 5b–e. The COF measured in test 1 is around 0.35 for all the four rails.

It is worth noticing that Fig. 5b, d show similar patterns, and Fig. 5c, d show similar patterns with more remarkable stick–slip. This study observes that in V-track the running bands of R2 and R4 are about 7 mm in width, a bit wider than those of R1 and R3, which are about 5 mm. Meanwhile, the measured wheel–rail dynamic contact behaviour,
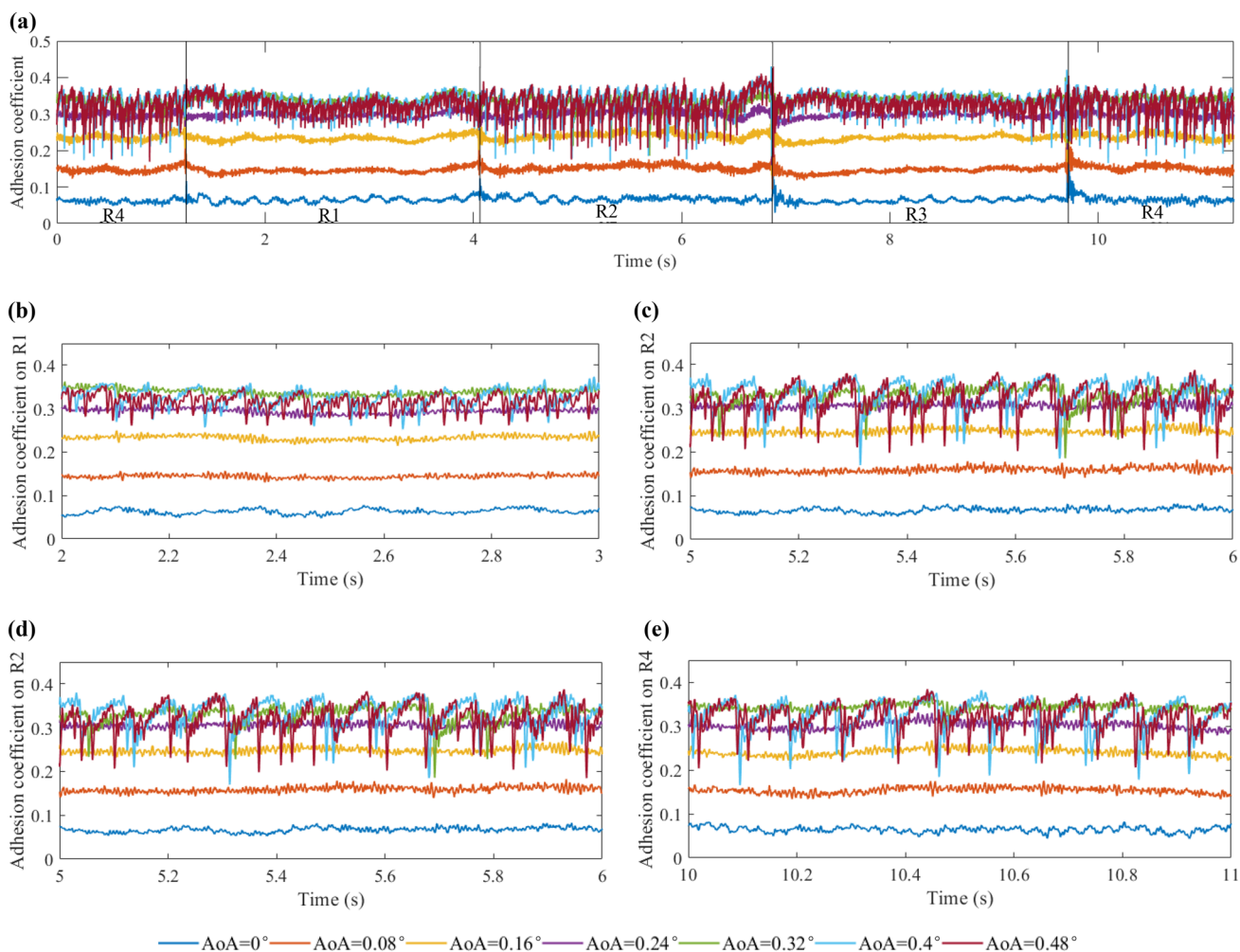

Fig. 5 The time histories of AC measured with a range of AoAs under the original dry condition (test 1): **a** an overview of the time histories over the ring rail; **b** a close-up of the ACs on R1; **c** a close-up of the ACs on R2; **d** a close-up of the ACs on R3; **e** a close-up of the ACs on R4

including the adhesion characteristics and contact-induced vibration, on R1 and R3 are quite similar, but may differ from those measured on R2 and R4. The possible reason is that the ring rail is not perfectly circular but slightly elliptical, leading to a symmetrical alignment of V-track.

Figure 6 shows the AC time histories measured with the increasing AoA with the application of 1 droplet of FM-A (test 4). The level of AC also increases with AoA but the increase is less considerable than that in the dry condition (test 1), suggesting that the application of FM-A may constrain the increase in AC induced by wheel curving motion. Comparing Figs. 5 and 6, a substantial reduction of AC level can be found at each AoA value after using FM-A. In addition, the stick–slip observed in test 1 disappears in test 4 with the application of FM-A, as shown more clearly in the close-ups of the measured AC time histories on each rail (see Fig. 15 in Appendix).

Figure 6. also shows that the AC keeps increasing with AoA even after the friction is saturated in test 4, indicating that FM-A is able to provide the positive friction characteristic to the wheel–rail interface as many other FMs [5, 9, 13]. The oxidation of the wheel–rail interface over time and consumption of FM during the cyclic wheel passages may also cause the increase in AC beyond friction saturation. These factors are proven to be negligible in this study, because each testing case shown in Table 1 was completed within 30 min, and the test at each AoA step took only about 10 test-run cycles, or wheel passages, to obtain good repeatability of at least three cycles in the desired

testing speed. The increase in AC beyond friction saturation, however, makes it difficult to determine its bound, namely COF. This study determines the COF based on that when the AC is approaching its bound, the increase in AC between two consecutive measurements with increasing AoA is very small, e.g. the yellow and purple curves plotted in Fig. 6b. In test 4, friction saturation is thus considered to be reached when the AoA is over 0.16°, and the COF is about 0.12, a bit higher than the safe limit for traction and braking, which is 0.1 [27].

After a careful clean of the wheel and rail interfaces, the ACs with the increasing AoA were measured again in the dry condition (test 5). As shown in Fig. 7, the COF obtained in test 5 is also approximately 0.35, meeting the level of COF in test 1. This ensures consistency and comparability of the results obtained on the two different testing days. Stick–slip also occurs in the dry contact condition in test 5, which can be more clearly observed in the close-ups of the measured AC time histories on each rail (see Fig. 16 in Appendix). In addition, apparent negative friction, i.e. the AC drops with the further increase in AoA beyond friction saturation, can be seen on R2 and R4 in Fig. 7.

FM-B was then applied to V-track. Figure 8 shows the time histories of AC measured with increasing AoA after using 1 droplet of FM-B in V-track (test 8). The increase in AC with AoA in test 8 is less significant than that in the dry conditions (test 1 and test 5) but more than that in the FM-A-treated condition (test 4). In addition, stick–slip disappears
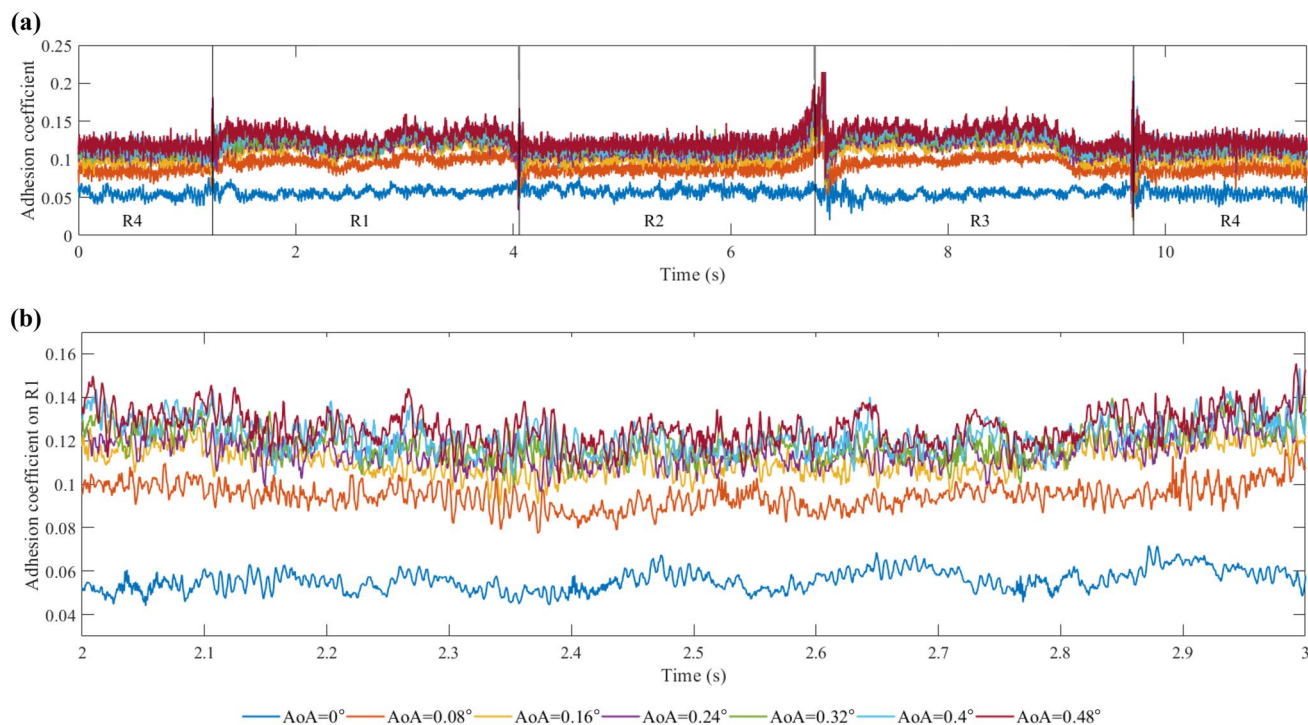

Fig. 6 The time histories of AC measured with a range of AoAs under the FM-A-treated condition (test 4): **a** overview of the time histories over the ring rail; **b** a close-up showing the very small increase in AC beyond friction saturation
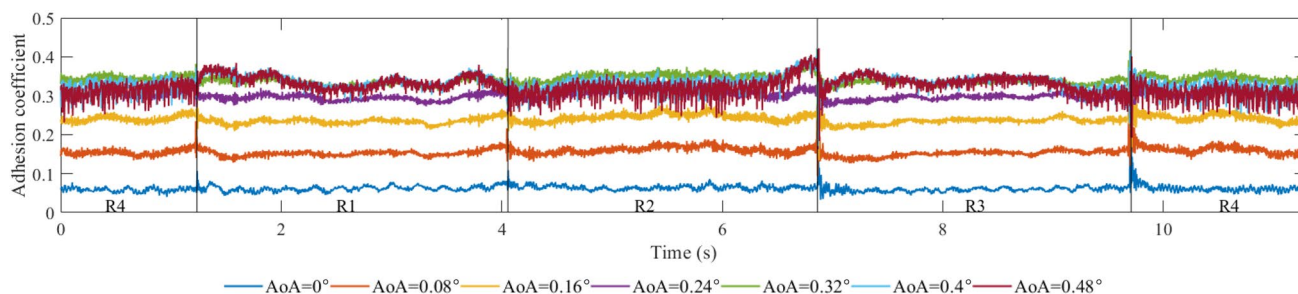
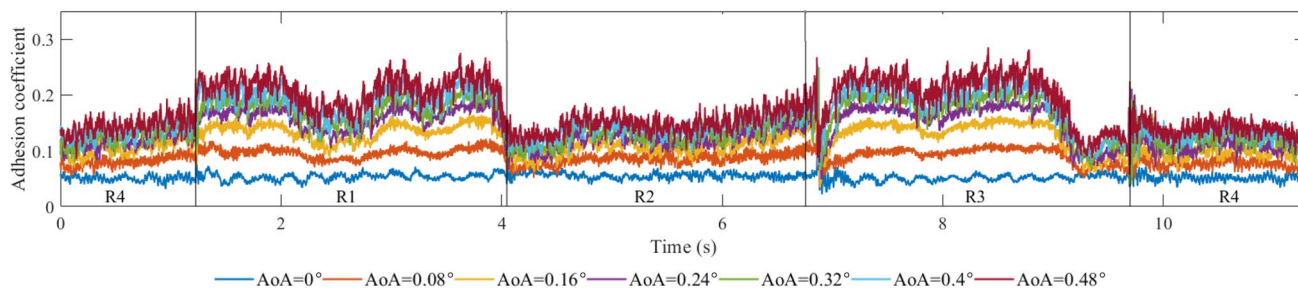**Fig. 7** The AC measured with a range of AoAs under the dry condition before using FM-B (test 5)

Fig. 8 The time histories of AC measured with a range of AoAs under the FM-B-treated condition (test 8)

on R2 and R4 with a drop of COF to about 0.16, but still takes place on R1 and R3 with a smaller drop of COF to about 0.22. As reported in [5], stick–slip may be eliminated by reducing the friction to a very low level. Because no stick–slip is observed under the FM-A-treated condition with the COF below 0.16, we may deduce that the threshold of the COF governing the occurrence of stick–slip in V-track ranges between 0.16 and 0.22. Moreover, the FMs reduce the adhesion level of R2 and R4 to a greater extent than R1 and R3, as shown in Figs. 6 and 8. That is probably associated with the difference in the width of the running band mentioned above: the running bands of R2 and R4 are a bit wider, and thus, a larger amount of FM may be consumed and take effect.

3.1.2 Influence on ABA under dry and FM-treated conditions

Regarding the ABA, same as the analysis of wheel–rail adhesion, the results measured on R1 and R3 are similar, and those on R2 and R4 are similar. Figure 9 shows the 1/3 octaves of the ABA measured on the four rails in the original dry condition (test 1). The measured ABAs in all three directions slightly increase with AoA before the friction saturation. When the friction is saturated, stick–slip occurs (AoA ≥ 0.4° for R1 and R3, and AoA ≥ 0.32° for R2 and R4, as shown in Fig. 5), and the measured ABAs increase dramatically in some frequency ranges: below 2 kHz and 5–6 kHz in the longitudinal ABA,

500 Hz–1.5 kHz in the vertical ABA, and below 2 kHz in the lateral ABA. Note that the normal load was kept constant in this study; the significant increase in ABA was, thus, caused by the change of friction. This indicates that the friction-induced vibration will not be remarkably increased during curving motion unless stick–slip contact occurs. A practical outcome of the results is that as long as the stick–slip is avoided, large-amplitude vibration and noise are expected to be eliminated at curved tracks. The ABA measured under the dry contact condition before using FM-B (test 5) shows the same trend, which can be found in Appendix (see Fig. 18).

When 1 droplet of the FMs was used in test 4 (for FM-A) and test 8 (for FM-B), the increase in ABA with AoA was less pronounced. In other words, ABA is less sensitive to variations in the AoA when the FMs are applied. The ABAs measured on R1 in tests 4 and 8 are shown in Figs. 10. The results on R2–R4 show the same trend, which can be found in Appendix (Figs. 19 and 20). When applying 1 droplet of FM-A, with the increase in AoA, a minor increase in the lateral ABA can be seen below 300 Hz; when applying 1 droplet of FM-B, the lateral ABA increases up to the frequency range of 800 Hz, remarkably for the cases of AoA ≥ 0.32° where stick–slip occurs, and an increase in the longitudinal ABA with AoA is noticeable below 100 Hz. These results indicate that the application of FM-A can effectively restrict the increase in wheel vibration during the curving motion. However, the application of FM-B seems to be less effective in terms of friction-induced
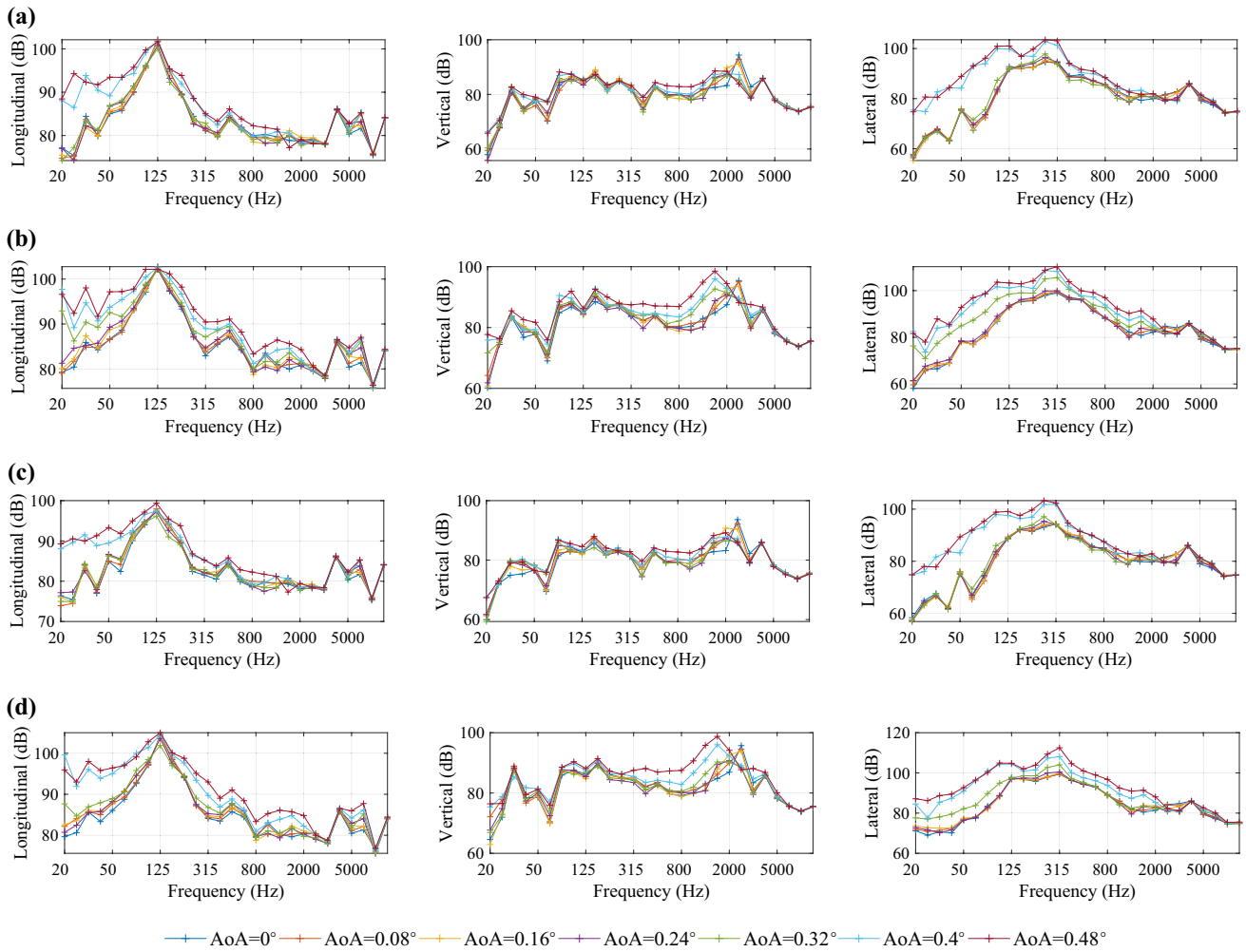
Fig. 9 The 1/3 octaves of the ABA measured with the increasing AoA under the original dry condition (test 1, from left to right: longitudinal, vertical, lateral ABA): **a** R1; **b** R2; **c** R3; **d** R4
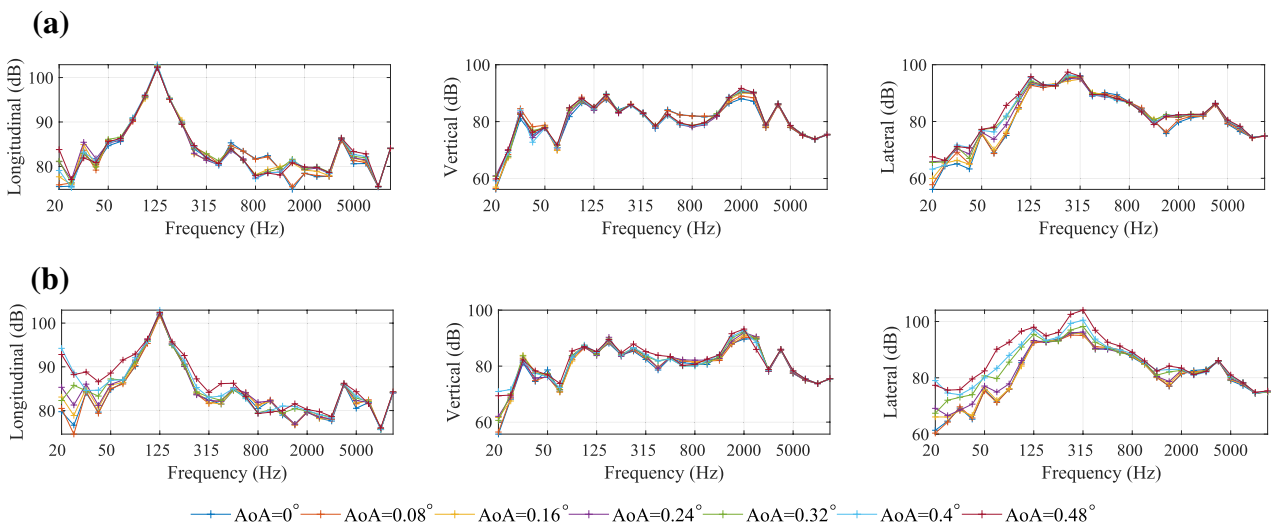

Fig. 10 The 1/3 octaves of the ABA measured with the increasing AoA under the FM-treated conditions (from left to right: longitudinal, vertical, lateral ABA): **a** with the application of FM-A (test 4); **b** with the application of FM-B (test 8)

vibration reduction, mainly because the stick–slip phenomenon is not eliminated. In comparison to the ABA measured under the dry conditions in test 1 (see Fig. 9) and test 5 (see Fig. 16 in Appendix), we may also conclude that ABA increases with AoA more significantly under the higher-COF condition than under the lower-COF condition. In addition, the analysis of the AoA-dependent ABA in this section indicates that the large AoA induces high-level vibration only when stick–slip takes place. The good correspondence between the ABA peaks and the sudden slip motion will be presented in a follow-up paper. Stick–slip induced by the large lateral creepage is thus expected to be detected by ABA measurements.

3.2 Influence of the FM dosage

A slight change in FM dosage may dramatically change the wheel–rail friction level [9]. This section investigates the influence of FM dosage on wheel–rail adhesion with various AoAs, and on ABA with small and large AoA, representing the friction-induced wheel vibration on straight tracks and sharp curves, respectively. As mentioned in Sect. 2.2 'Test procedure', the dosages of FM used in this study are 1/4, 1/2 and 1 droplet per V-track circle.

3.2.1 Influence on wheel–rail adhesion with different AoAs

The AC–AoA relationships, i.e. wheel–rail adhesion as a function of AoA, on the four rails of V-Track influenced by FMs with different dosages are plotted in Fig. 11. Despite the equivalence of AoA to the lateral creepage in the steady state, the AC–AoA relationship rather than the term lateral creep curve is used because the longitudinal creepage induced by the driven wheel is not negligible in this study. As shown in Fig. 11, the traction coefficient, i.e. the AC with zero-AoA, is not zero but around 0.06. A trailing wheel with small longitudinal force is thus simulated in this study. Figure 11 also shows that with the increase in the dosage of the FMs applied the adhesion level as well as the COF decreases, more significantly by FM-A. The AC reaches the COF, i.e. friction saturation is achieved, when AoA $\geq 0.32°$ in the dry contact tests (tests 1 and 5), AoA $\geq 0.24°$ in the FM-B-treated contact tests (tests 6–8) and AoA $\geq 0.16°$ in the FM-A-treated contact tests (tests 2–4), which is identified by obvious stick–slip oscillation for the dry contact and FM-B-treated cases (tests 1 and 5–8), and by the very slight increase in AC for the FM-A-treated cases (tests 2–4), as explained in Sect. 3.1.1. The COFs measured under the dry contact conditions are around 0.35, and those for the
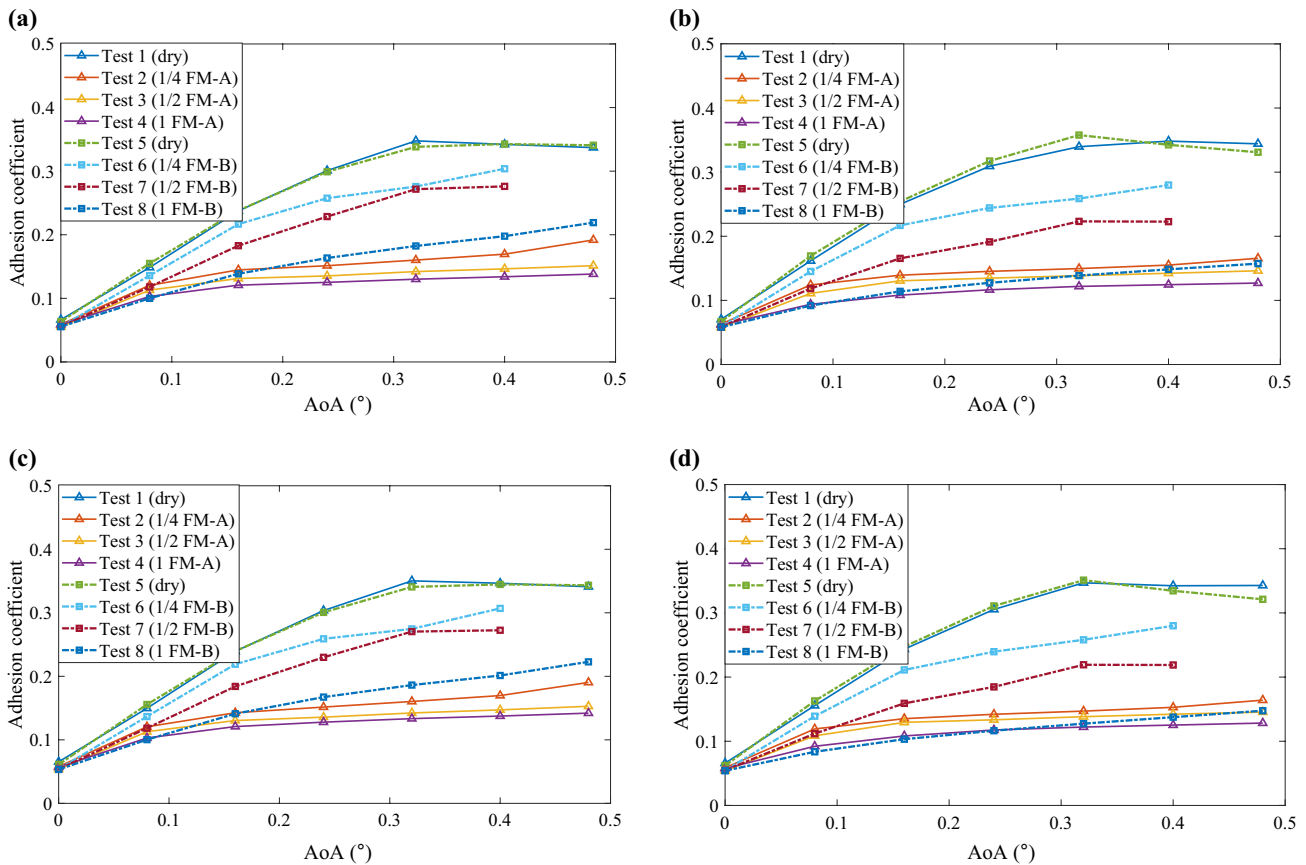

Fig. 11 The AC–AoA relationship influenced by the FMs with different dosages: **a** R1; **b** R2; **c** R3; **d** R4

FM-treated conditions range between 0.1 and 0.26, which are basically in line with the friction range reported in [10]. Note that these values can only be taken as a qualitative indication of the actual wheel–rail situation because of the differences in the test set-up, as outlined in [10, 24, 28]. The negative friction, i.e. friction saturation is followed by a decreasing slope, occurs in the dry conditions and is changed to positive with the applications of the FMs, corresponding well to results reported in some other FM studies [2, 9, 24].

With the applications of the FMs, the adhesion level can be more significantly reduced in the larger-AoA cases. When the AoA is nominally zero, the adhesion is mainly provided by the longitudinal force, the reduction of AC by using FM is about 12% (from 0.065 to 0.057), as shown in Fig. 12, which plots the time histories of AC on R1 when AoA = 0°. The results of R2–R4 showing the same trend can be found in Appendix (Fig. 21). The zero-AoA test may represent the case of a train traveling on a straight track. Corresponding to the reduction of AC, reductions of traction force and the related energy consumption can be expected [29]. When the AoA increases to 0.32°, friction saturation is achieved for all the eight testing cases. The AC is reduced to about 60% (from 0.35 to 0.13) by using 1 droplet of FM-A and about 50% (from 0.35 to 0.17) by using 1 droplet of FM-B. This is thought to be representative of a train passing a curve. Therefore, with the application of the FMs at curves, the friction level and force can be reduced, but note that the threshold of friction saturation in terms of AoA is also reduced, e.g. from AoA = 0.32° for the dry contact to AoA = 0.24° or even 0.16 for the FM-treated contact, which increases the likelihood of wheel sliding.

Comparing the time histories of AC influenced by the dosage of FM with a large AoA (AoA = 0.4°) in Fig. 13, friction saturation can be identified by obvious stick–slip oscillation for the dry and FM-B cases (tests 1 and 5–8). When FM-A is used (tests 2–4), stick–slip disappears although friction saturation has been achieved, which can be identified by the very slight increase in AC with AoA, as explained in Sect. 3.1.1. The FM-A-treated COF ranges between 0.12 and 0.16, still falling in the range of 'normal adhesion' [30]. Figure 13 also

shows that the increase in the FM-A dosage from 1/4 to 1 droplet takes less pronounced effects in the adhesion reduction. As reported in [9], the increasing application of FM beyond a limit has an insignificant effect and no benefit. To achieve cost-efficiency and to avoid low adhesion and track contamination, 1/4 droplet of FM-A may be an optimal dosage for friction reduction in V-track.

The AC levels measured with different dosages of FM-B in tests 6–8 have relatively large differences. Stick–slip was not eliminated but surprisingly intensified to some extent when 1/4 or 1/2 droplet of FM-B was used although the friction level decreased, especially on R1 and R3, as shown in Fig. 13b and d, respectively. A sufficient supply of FM-B should thus be guaranteed in practice to reduce the friction level and avoid large stick–slip. Same as the results shown in Sect. 3.1.1, Fig. 13 shows that the threshold of COF governing the occurrence of stick–slip ranges between 0.16 and 0.22. In other words, stick–slip may take place in V-track when the COF is over 0.22, and disappears when the COF is below 0.16.

Figure 11 shows that FM-B changes the negative friction characteristic of the wheel–rail interface to positive, while Fig. 13 shows stick–slip was not eliminated by using FM-B. We may thus conclude that the negative friction, as an underlying cause of stick–slip, is not a must for stick–slip. Stick–slip may occur and even be intensified although the negative friction is changed to positive by FM. An analysis of the mechanism of FM on the occurrence of stick–slip will be presented in a follow-up paper.

3.2.2 Influence on ABA with small and large AoAs

This section discusses the friction-induced ABA influenced by the FM dosage. Figure 14 compares the 1/3 octaves of ABA measured on R1 and R2 with small (AoA = 0°) and large (AoA = 0.4°) AoAs. The results of R3 and R4 show the same trends as those of R1 and R2, which be found in Appendix (Figs. 22 and 23, respectively). When the AoA is small, the 1/3 octaves of the ABA (dotted curves in Fig. 14) measured in all the testing cases basically overlap with each
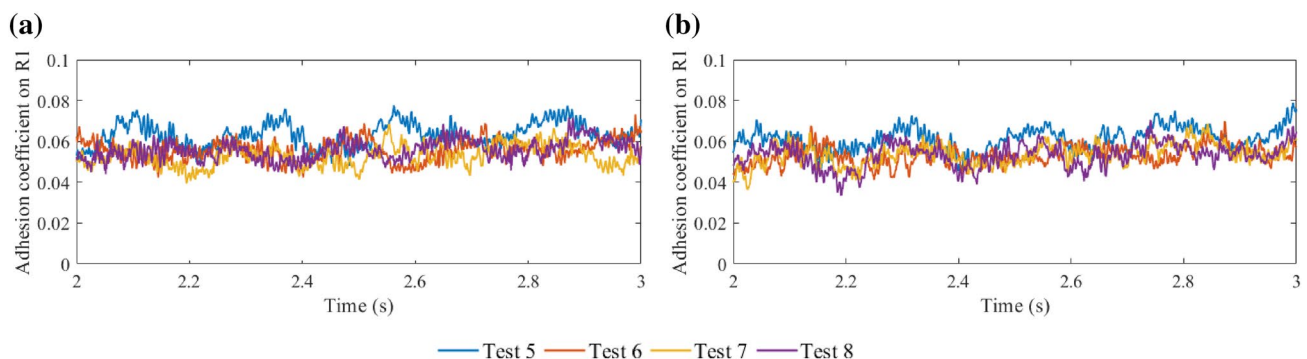

Fig. 12 The AC of R1 affected by the FM dosage when AoA = 0°: **a** effects of the FM-A dosage; **b** effects of the FM-B dosage

(a)

(b)

(c)

(d)

(e)

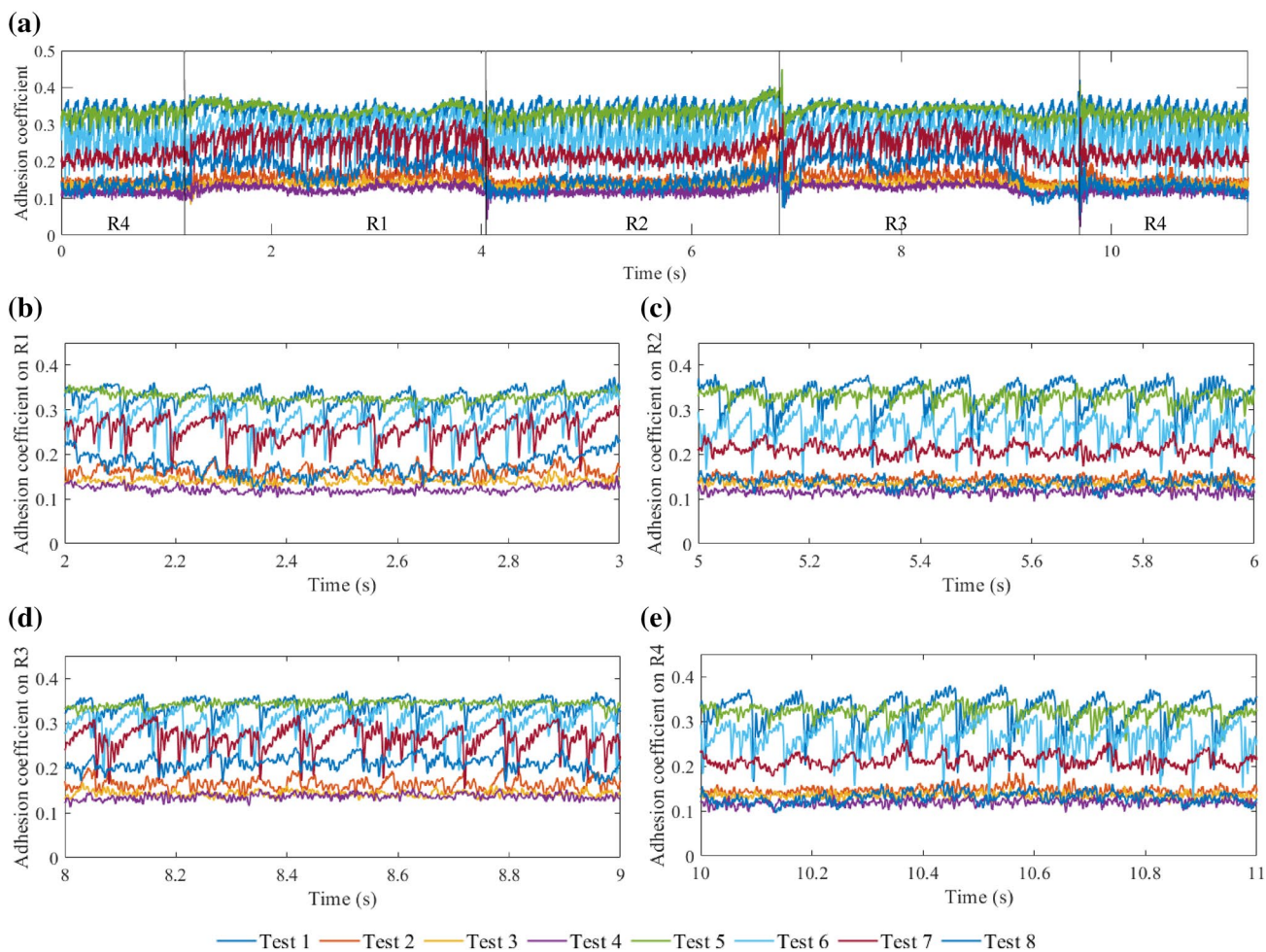— Test 1 — Test 2 — Test 3 — Test 4 — Test 5 — Test 6 — Test 7 — Test 8

Fig. 13 The AC affected by the FM dosage when AoA = 0.4°: **a** an overview of the AC time histories over the ring rail; **b** a close-up of the ACs on R1; **c** a close-up of the ACs on R2; **d** a close-up of the ACs on R3; **e** a close-up of the ACs on R4

other, indicating the application of the FMs and their dosages play a trivial role in the ABA reduction when the creepage is small.

When the AoA is large, with the application of FM-A (the dash-dotted curves in Fig. 14a, b), the longitudinal and lateral ABA considerably decrease below 2 kHz, and the vertical ABA slightly decreases in the frequency range of 600 Hz–1 kHz. Because these frequency components of ABA increase with AoA in the dry contact, as analysed in Sect. 3.1.2, we may again conclude that the application of FM-A can effectively restrict the increase in wheel vibration during the curving motion. Furthermore, the dosage of FM-A influences its effectiveness on the ABA reduction, more remarkably on R1 and R3: the reduction of the longitudinal and lateral ABA with the application of 1/4 droplet of FM-A (test 2) is smaller than that using 1/2 or 1 droplet (tests 3 and 4). By using 1/2 droplet, or more, of FM-A, the ABA measured with AoA = 0.4° can be suppressed to the level measured with AoA = 0°. It can thus be concluded that

the optimal dosage of FM-A for vibration reduction is 1/2 droplet per V-track circle.

The application of FM-B may, however, increase the ABA level when the AoA is large (the dash-dotted curves in Fig. 14c, d). The ABAs were increased on R1 and R3 by using FM-B with all the three dosages (tests 6–8), and on R2 and R4 when 1/4 droplet of FM-B was applied (test 6). Note that all the testing cases with the ABA increase are accompanied by the stick–slip intensification, as shown in Fig. 13. The analysis of FM-B suggests that the reduction of friction level may not necessarily result in the reduction of vibration level. The oscillation frequency of the friction force and the wheel/rail structural dynamic behaviour should be also considered in the control of friction-induced vibration. Considering that the FM-B-treated condition reaches friction saturation at a smaller AoA than the untreated condition (see Fig. 11) and a small dosage of FM-B may intensify stick–slip, a continuous and sufficient supply of FM-B to wheel–rail interfaces should
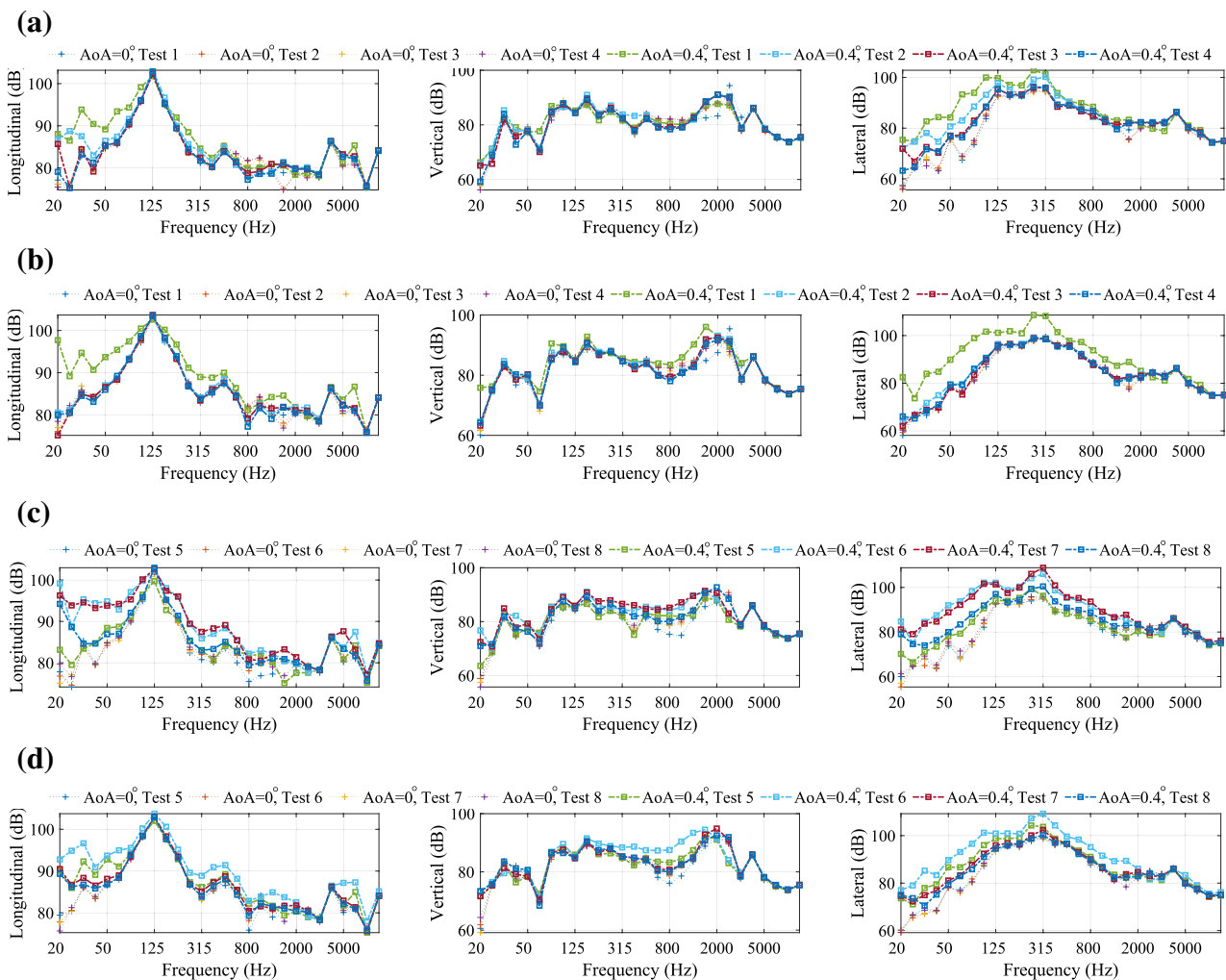
(a)

(b)

(c)

(d)

Fig. 14 The 1/3 octaves of the measured ABAs influenced by the FM dosage with small and large AoA (from left to right: longitudinal, vertical, lateral ABA): **a** ABA on R1 with the application of FM-A; **b** ABA on R2 with the application of FM-A; **c** ABA on R1 with the application of FM-B; **d** ABA on R2 with the application of FM-B

be guaranteed in practice to avoid the large-amplitude stick–slip and consequent vibration and noise.

4 Discussion and future work

When comparing the wheel–rail frictional behaviour under the dry contact conditions (ACs displayed in Figs. 5 and 7), we may see that although both COFs are approximately 0.35, differences in frictional behaviour exist close to and during the friction saturation. On the one hand, more significant stick–slip occurred in test 1 (Fig. 5) than in test 5 (Fig. 7): on R2 and R4, the ACs dropped from 0.35 to 0.2 in test 1 but to 0.25 in test 5 when slip occurred; on the other hand, test 5 presents a more remarkable negative friction characteristic: the COF dropped from 0.35 to 0.33 beyond the friction

saturation in test 5 but to 0.34 in test 1. These differences suggest that the wheel–rail frictional contact behaviour close to and beyond friction saturation may not be sufficiently represented by the ratio of tangential force and normal load, i.e. AC. Other factors that may influence the frictional behaviour and performance of FMs applied, such as the roughness level of the wheel–rail interface, should be studied in future work.

In addition, this study shows that the water-based FM-A caused lower friction levels than the oil-based FM-B, while the conflicting results are reported in some other studies, e.g. in [15]. The water-based FM may generate a lower friction level when the water in it is insufficiently vaporised. This is, however, not the case in this study. To handily measure the weight loss and determine the volatilisation process of the water-based FM-A tested in this study, we used the bulk samples of the FM. It showed that the FM-A sample 'stabilised' in 2 h with a weight loss of 1.4%. Since the

volatilisation process is expected to be shorter when the FMs are spread onto the rail top as a thin layer, and the FM-treated tests were conducted 2 h after the FM application, the water-based FM-A should have been 'prepared' for the tests. The comparisons of the effects of the water-based and oil-based FMs thus deserve further investigations.

5 Conclusions

This study employs the V-track test rig to investigate the effects of two types of FM on wheel–rail dynamic interactions with various AoAs, i.e. under various adhesion conditions. The influences of AoA and FM dosage on wheel–rail adhesion characteristics and frictional rolling induced ABA are analysed. Aiming to provide new insights into the proper applications of FM, this study yields the following conclusions:

1. Regarding the influence of AoA

- Friction saturation is achieved by the step-by-step increase in AoA in V-track.
- Friction saturation can be identified by the occurrence of stick–slip in the dry and FM-B-treated conditions, and by the small increase in adhesion level between two consecutive measurements with increasing AoA in the FM-A-treated condition.
- The increase in ABA with AoA is not remarkable until stick–slip occurs, suggesting that the high-level vibration induced by the large AoAs in the curved tracks can be avoided by eliminating stick–slip, and the stick–slip induced by the large lateral creepage is expected to be detected by ABA tests.

2. Regarding the FM application

- The adhesion and friction levels in V-track are reduced by both types of FM, more significantly by FM-A when the same dosage is used.
- The negative friction characteristic occurs in the dry contact condition in V-track and is changed to positive with the applications of the FMs.
- The application of FM-A may effectively avoid stick-slip and is thus promising for the simultaneous mitigation of interface deterioration, friction-induced unstable vibration and noise.
- The optimal dosages of FM-A for friction and vibration reduction are 1/4 droplet and 1/2 droplet per V-Track circle, respectively.
- The application of FM-B fails to eliminate stick-slip despite the fact that it changes the negative friction to positive. This indicates negative friction is not a must for stick-slip.
- Applying a small dosage of FM-B (e.g. 1/4 or 1/2 droplet per V-track circle) may intensify stick-slip contact and consequently increase ABA although the friction level is decreased. A sufficient supply of FM-B should thus be guaranteed in the real-life application.

Appendix

See Figs. 15, 16, 17, 18, 19, 20, 21, 22 and 23

(a)

(b)

(c)

(d)

(e)

AoA=0° AoA=0.08° AoA=0.16° AoA=0.24° AoA=0.32° AoA=0.4° AoA=0.48°
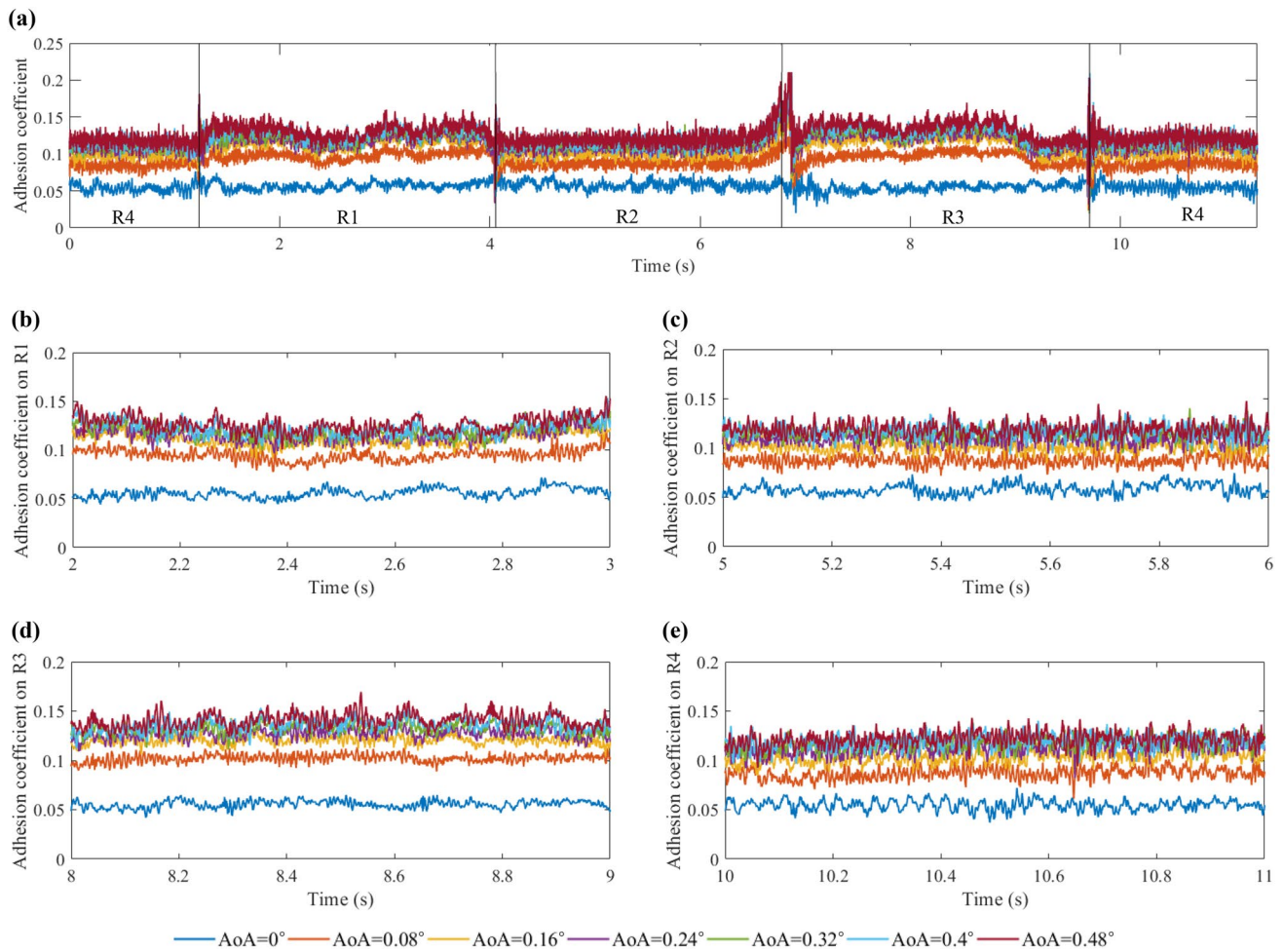
Fig. 15 The time histories of AC measured with a range of AoAs under the FM-A-treated condition (test 4): **a** an overview of the time histories over the ring rail; **b** a close-up of the ACs on R1; **c** a close-up of the ACs on R2; **d** a close-up of the ACs on R3; **e** a close-up of the ACs on R4
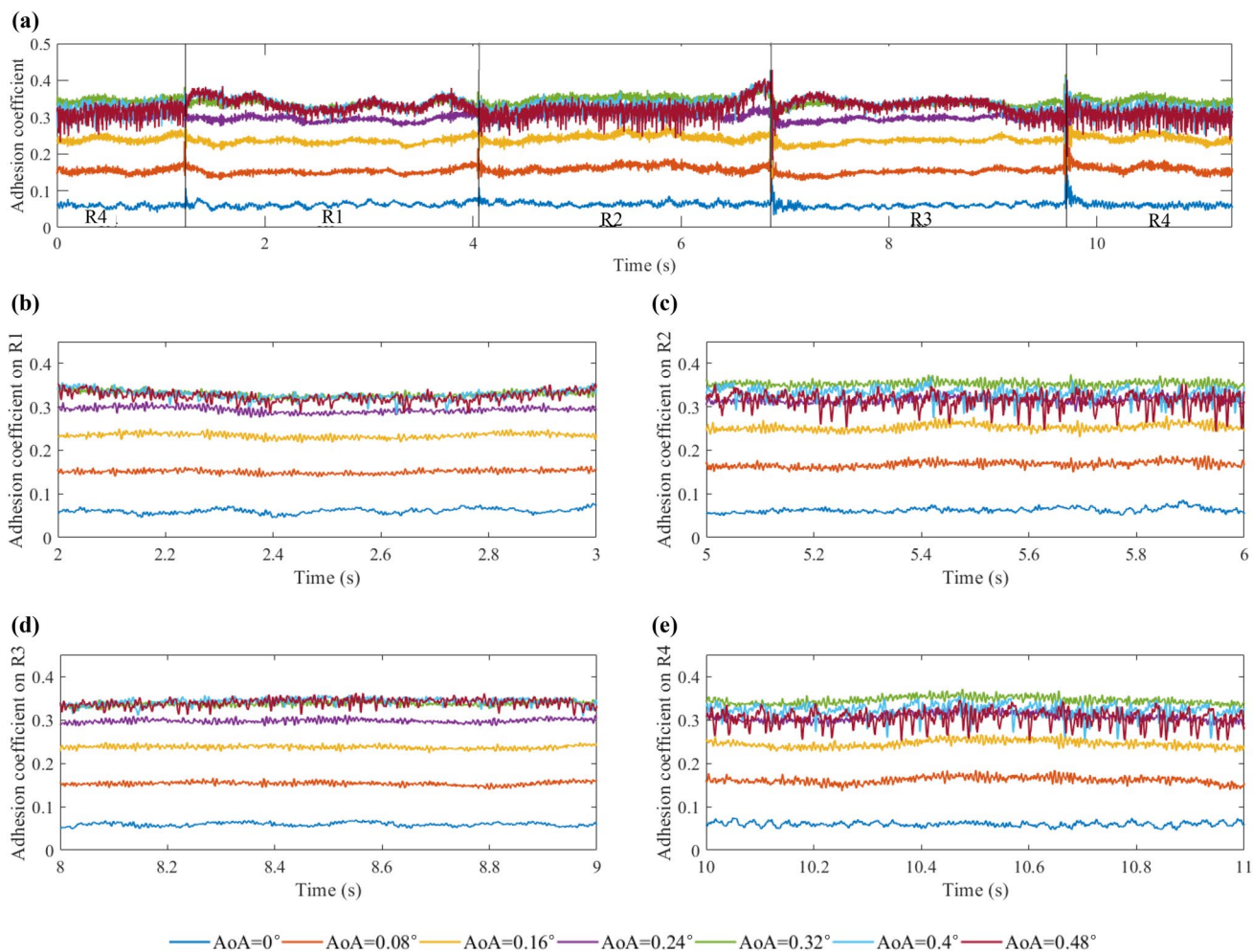
(a)

(b)

(c)

(d)

(e)

AoA=0° AoA=0.08° AoA=0.16° AoA=0.24° AoA=0.32° AoA=0.4° AoA=0.48°

Fig. 16 The time histories of AC measured with a range of AoAs under the dry condition before using FM-B (test 5): **a** an overview of the time histories over the ring rail; **b** a close-up of the ACs on R1; **c** a close-up of the ACs on R2; **d** a close-up of the ACs on R3; **e** a close-up of the ACs on R4
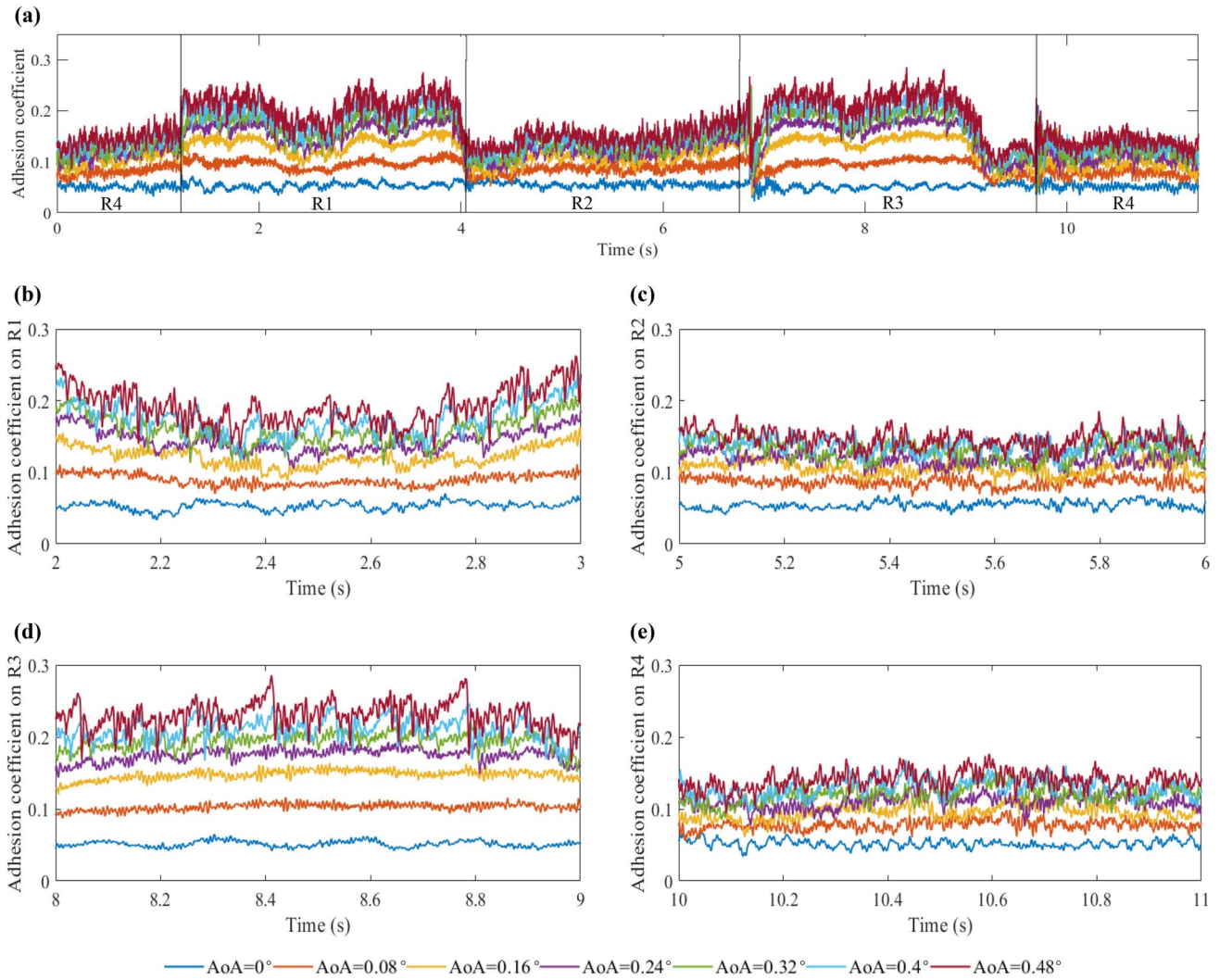
Fig. 17 The time histories of AC measured with a range of AoAs under the FM-B-treated condition (test 8): **a** an overview of the time histories over the ring rail; **b** a close-up of the ACs on R1; **c** a close-up of the ACs on R2; **d** a close-up of the ACs on R3; **e** a close-up of the ACs on R4
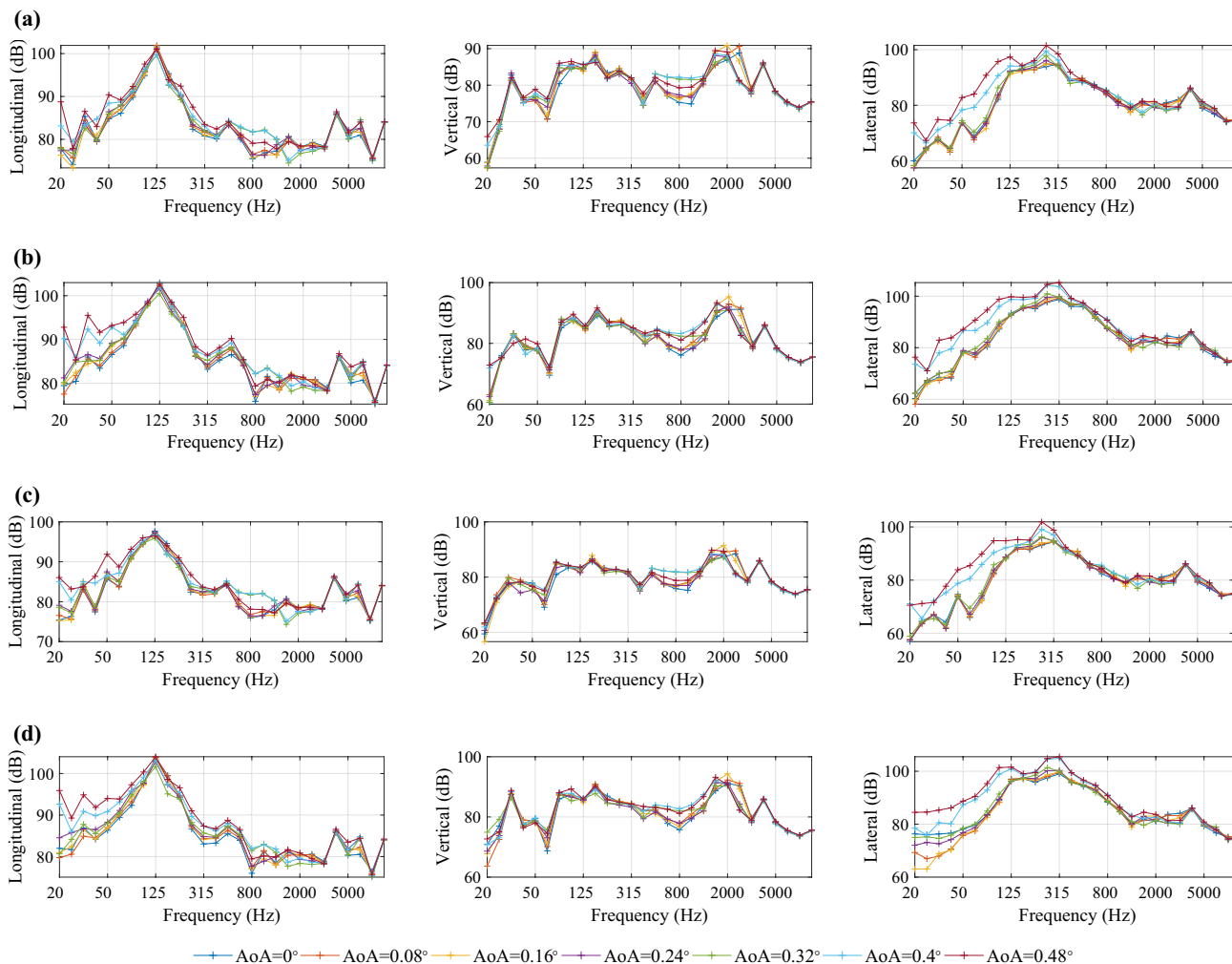
Fig. 18 The 1/3 octaves of the ABA measured with the increasing AoA under the dry condition before using FM-B (test 5, from left to right: longitudinal, vertical, lateral ABA): **a** R1; **b** R2; **c** R3; **d** R4
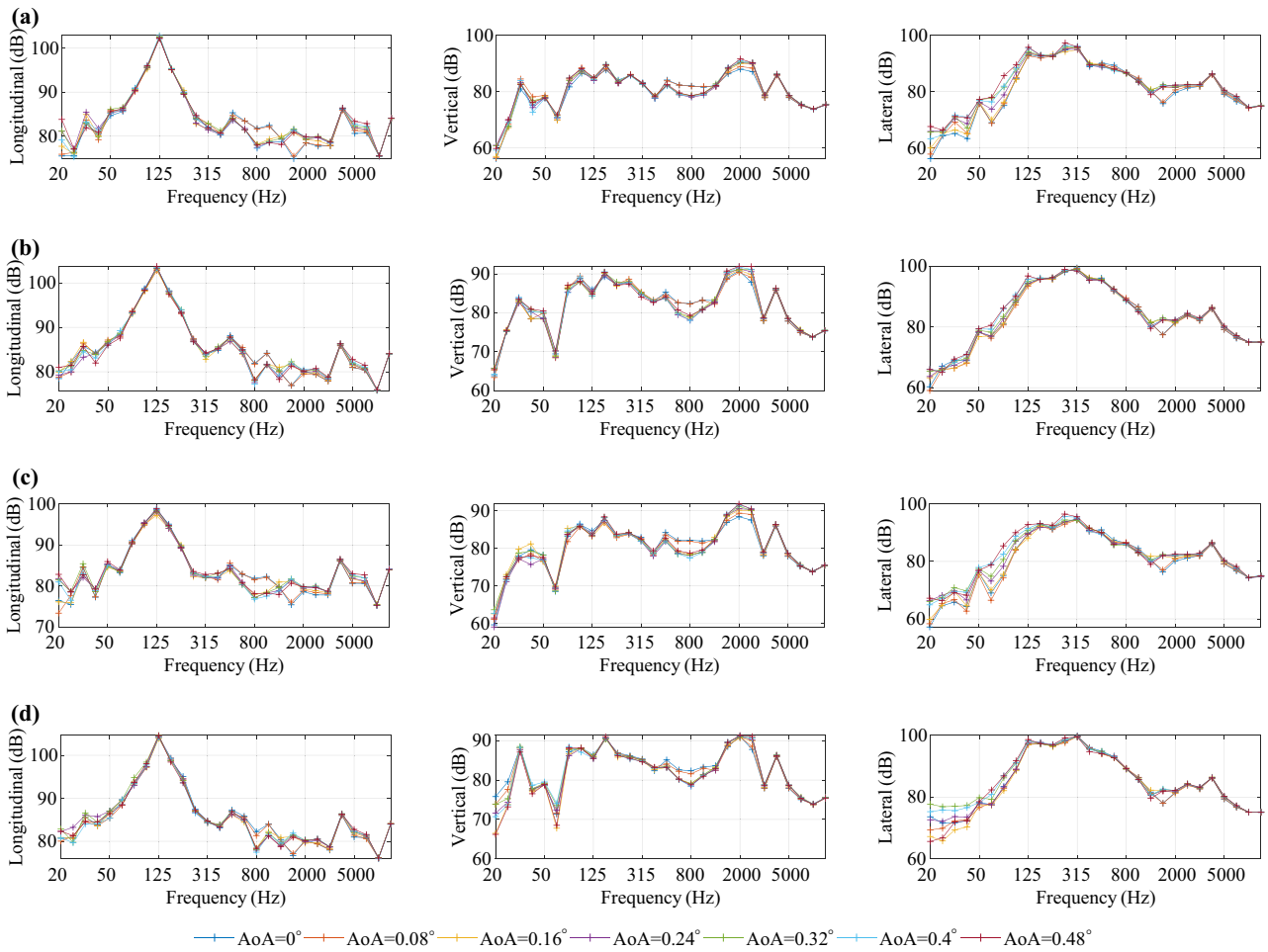
Fig. 19 The 1/3 octaves of the ABA measured with the increasing AoA under the FM-A-treated conditions (test 4, from left to right: longitudinal, vertical, lateral ABA): **a** R1; **b** R2; **c** R3; **d** R4
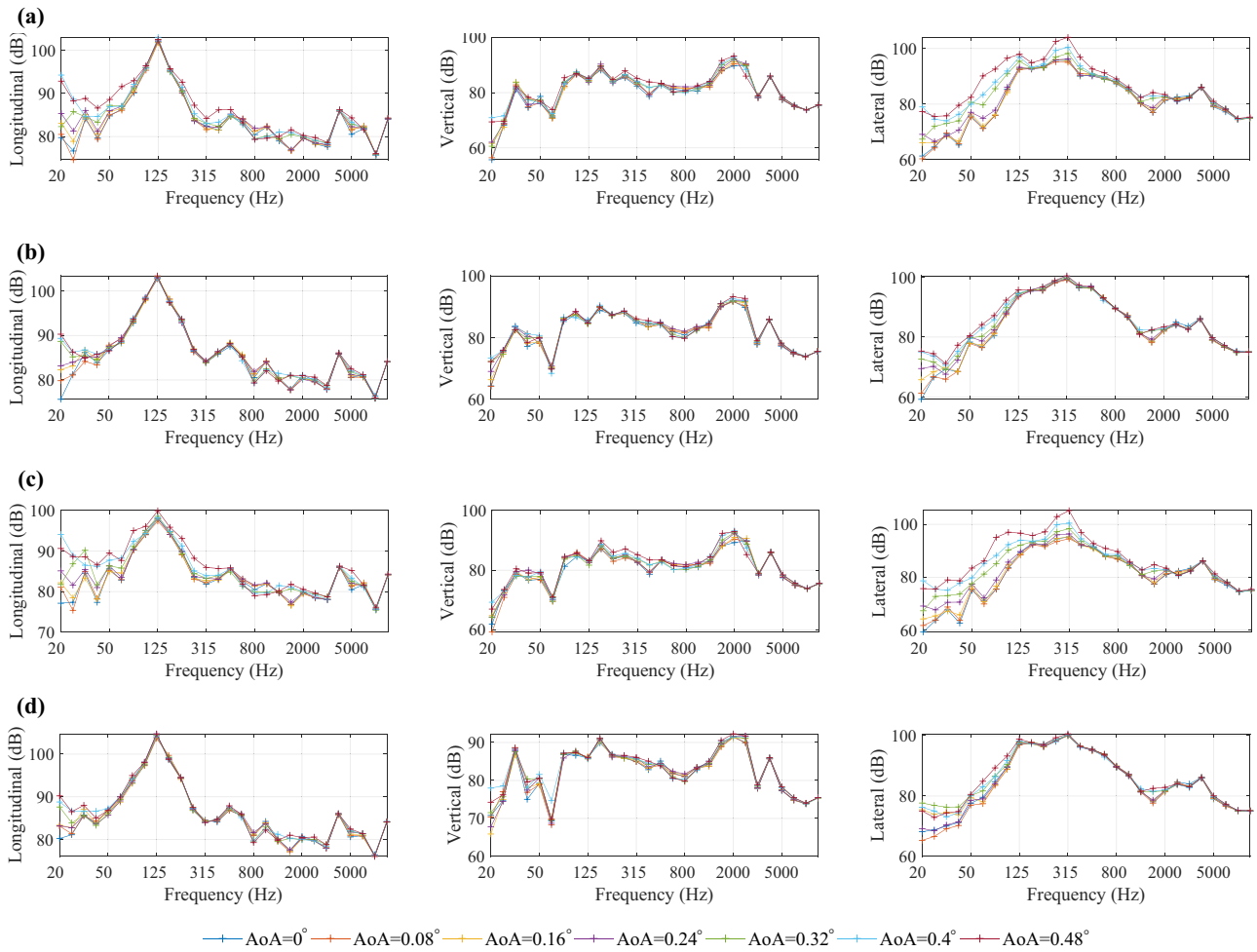
Fig. 20 The 1/3 octaves of the ABA measured with the increasing AoA under the FM-B-treated conditions (test 8, from left to right: longitudinal, vertical, lateral ABA): **a** R1; **b** R2; **c** R3; **d** R4
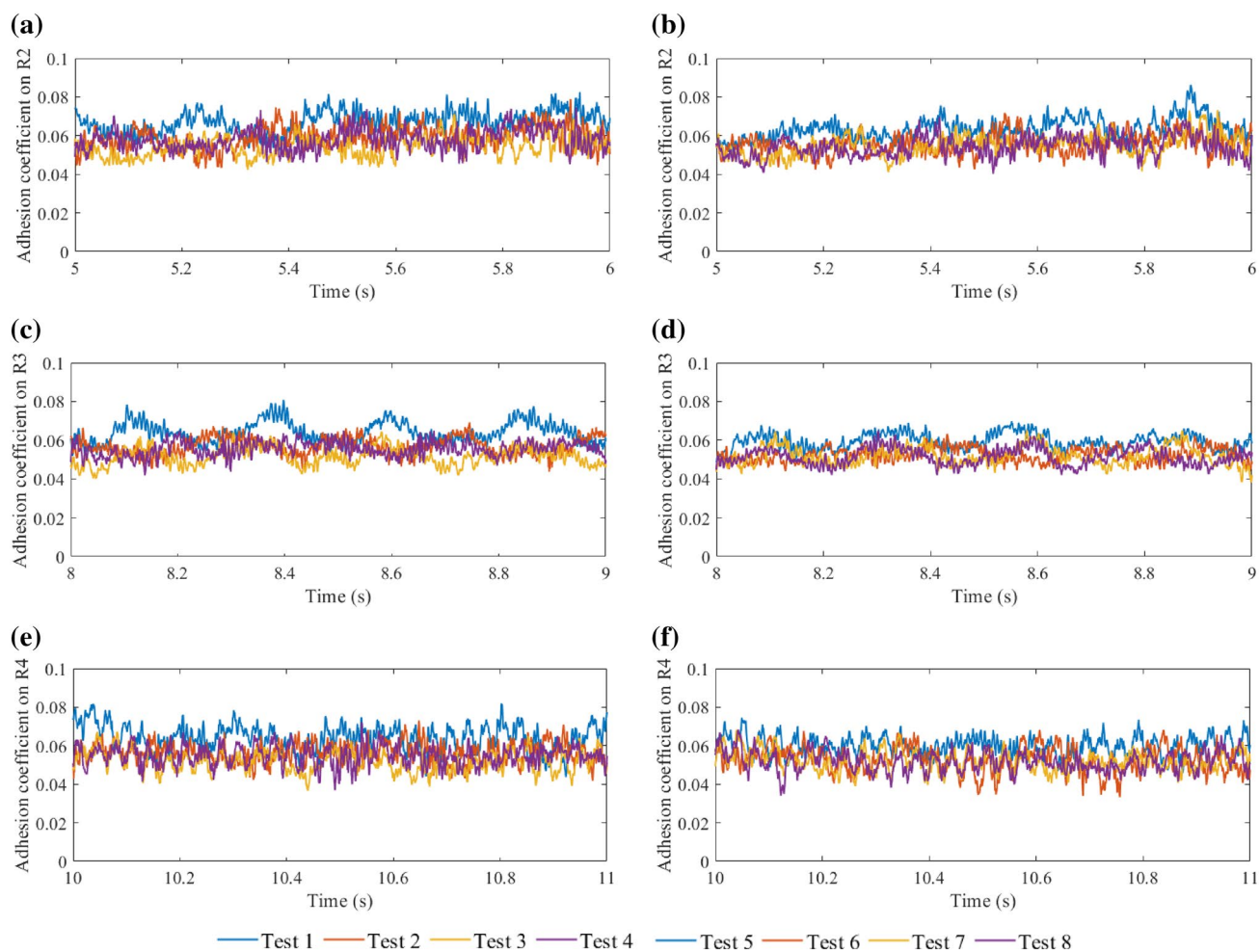
Fig. 21 The AC of R1 affected by the FM dosage when AoA = 0°: **a** FM-A test on R2; **b** FM-B test on R2; **c** FM-A test on R3; **d** FM-B test on R3; **e** FM-A test on R4; **f** FM-B test on R4

Fig. 22 The 1/3 octaves of the measured ABAs influenced by the FM-A dosage with small and large AoA (from left to right: longitudinal, vertical, lateral ABA): **a** on R1; **b** on R2; **c** on R3; **d** on R4

(a)

(b)

(c)

(d)

······ AoA=0.° Test 5 ···+··· AoA=0.° Test 6 ······ AoA=0.° Test 7 ···+··· AoA=0.° Test 8 --□-- AoA=0.4.° Test 5 --□-- AoA=0.4.° Test 6 --■-- AoA=0.4.° Test 7 --■-- AoA=0.4.° Test 8
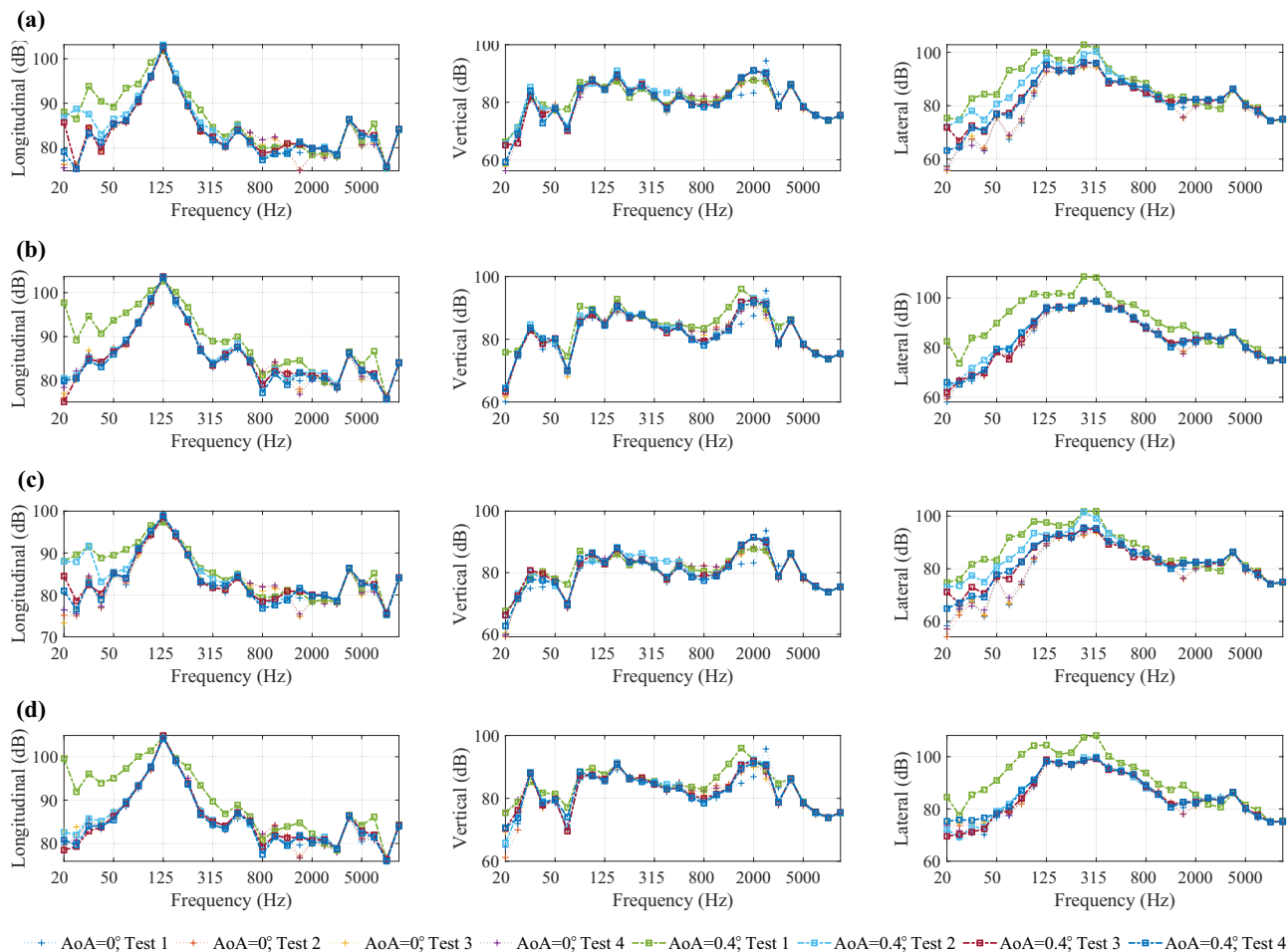
Fig. 23 The 1/3 octaves of the measured ABAs influenced by the FM-B dosage with small and large AoA (from left to right: longitudinal, vertical, lateral ABA): **a** on R1; **b** on R2; **c** on R3; **d** on R4
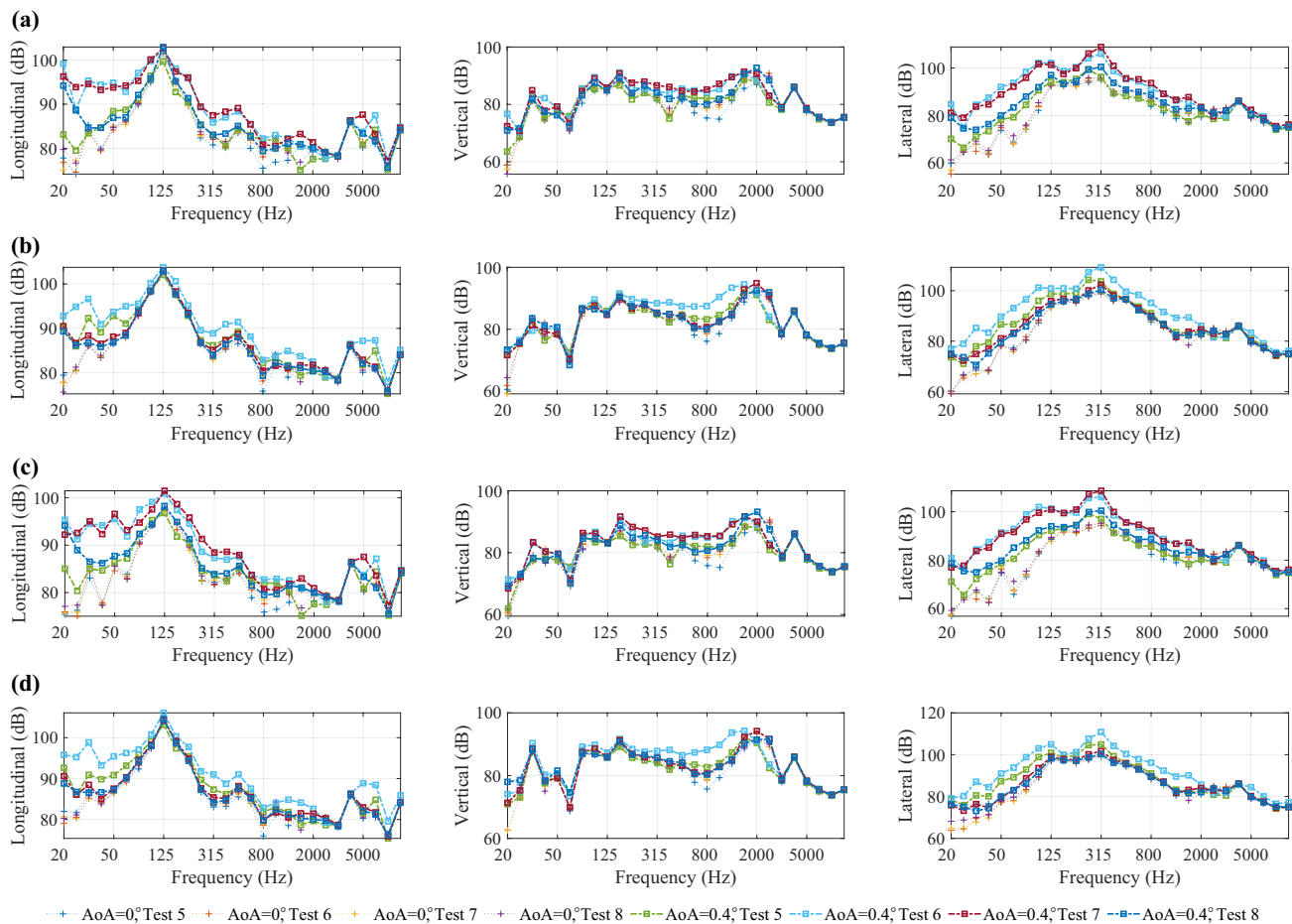
References

1. Li Z, Arias-Cuevas O, Lewis R, Gallardo-Hernández EA (2008) Rolling-Sliding laboratory tests of friction modifiers in leaf contaminated wheel–rail contacts. Tribol Lett 33(3–4):97–109

2. Arias-Cuevas O, Li Z, Lewis R, Gallardo-Hernández EA (2010) Rolling-Sliding laboratory tests of friction modifiers in dry and wet wheel–rail contacts. Wear 268(3–4):543–551

3. Eadie DT, Elvidge D, Oldknow K, Stock R, Pointner P, Kalousek J, Klauser P (2008) The effects of top of rail friction modifier on wear and rolling contact fatigue: full-scale rail–wheel test rig evaluation, analysis and modelling. Wear 265(9–10):1222–1230

4. Idárraga Alarcón G, Burgelman N, Meza JM, Toro A, Li Z (2015) The influence of rail lubrication on energy dissipation in the wheel/rail contact: a comparison of simulation results with field measurements. Wear 330–331:533–539

5. Eadie DT, Kalousek J, Chiddick KC (2002) The role of high positive friction (HPF) modifier in the control of short pitch corrugations and related phenomena. Wear 253(1–2):185–192

6. Eadie DT, Santoro M, Kalousek J (2005) Railway noise and the effect of top of rail liquid friction modifiers: changes in sound and vibration spectral distributions in curves. Wear 258(7–8):1148–1155

7. Eadie DT, Santoro M, Oldknow K, Oka Y (2008) Field studies of the effect of friction modifiers on short pitch corrugation generation in curves. Wear 265(9–10):1212–1221

8. Yang Z, Deng X, Li Z (2019) Numerical modeling of dynamic frictional rolling contact with an explicit finite element method. Tribol Int 129:214–231

9. Harmon M, Lewis R (2016) Review of top of rail friction modifier tribology. Tribol—Mater Surf Interfaces 10(3):150–162

10. Areiza YA, Garcés SI, Santa JF, Vargas G, Toro A (2015) Field measurement of coefficient of friction in rails using a hand-pushed tribometer. Tribol Int 82(Part B):274–279

11. Spiryagin M, Wu Q, Polach O et al (2022) Problems, assumptions and solutions in locomotive design, traction and operational studies. Railw Eng Sci. https://doi.org/10.1007/s40534-021-00263-w

12. Matsumoto A, Sato Y, Ohno H et al (2005) Improvement of bogie curving performance by using friction modifier to rail/wheel interface. Wear 258(7–8):1201–1208

13. Eadie DT, Santoro M, Powell W (2003) Local control of noise and vibration with KELTRACK™ friction modifier and Protector® trackside application: an integrated solution. J Sound Vib 267(3):761–772

14. Liu X, Meehan PA (2016) Investigation of squeal noise under positive friction characteristics condition provided by friction modifiers. J Sound Vib 371:393–405

15. Stock R, Stanlake L, Hardwick C, Yu M, Eadie D, Lewis R (2016) Material concepts for top of rail friction management: classification, characterisation and application. Wear 366–367:225–232

16. Lewis SR, Lewis R, Evans G, Buckley-Johnstone LE (2014) Assessment of railway curve lubricant performance using a twin-disc tester. Wear 314(1–2):205–212

17. Naeimi M, Li Z, Petrov RH, Sietsma J, Dollevoet R (2017) Development of a new downscale setup for wheel–rail contact experiments under impact loading conditions. Exp Tech 42(10):1–17

18. Shrestha S, Spiryagin M, Wu Q (2020) Real-time multibody modeling and simulation of a scaled bogie test rig. Railw Eng Sci 28(2):146–159

19. Tao G, Wen Z, Jin X, Yang X (2020) Polygonisation of railway wheels: a critical review. Railw Eng Sci 28(4):317–345

20. Zhang P, Moraal J, Li Z (2021) Design, calibration and validation of a wheel-rail contact force measurement system in V-Track. Measurement 175:109105

21. de Beer FG, Janssens MHA, Kooijman PP (2003) Squeal noise of rail-bound vehicles influenced by lateral contact position. J Sound Vib 267(3):497–507

22. Baek K-S, Kyogoku K, Nakahara T (2008) An experimental study of transient traction characteristics between rail and wheel under low slip and low speed conditions. Wear 265(9–10):1417–1424

23. Chen H, Namura A, Ishida M, Nakahara T (2016) Influence of axle load on wheel/rail adhesion under wet conditions in consideration of running speed and surface roughness. Wear 366–367:303–309

24. Gallardo-Hernandez EA, Lewis R (2008) Twin disc assessment of wheel/rail adhesion. Wear 265(9–10):1309–1316

25. Fletcher DI, Lewis S (2013) Creep curve measurement to support wear and adhesion modelling, using a continuously variable creep twin disc machine. Wear 298–299:57–65

26. Monk-Steel AD, Thompson DJ, de Beer FG, Janssens MHA (2006) An investigation into the influence of longitudinal creepage on railway squeal noise due to lateral creepage. J Sound Vib 293(3–5):766–776

27. Lewis SR, Lewis R, Richards P, Buckley-Johnstone LE (2014) Investigation of the isolation and frictional properties of hydrophobic products on the rail head, when used to combat low adhesion. Wear 314(1–2):213–219

28. Olofsson U, Lyu Y (2017) Open system tribology in the wheel–rail contact—a literature review. Appl Mech Rev 69(6):060803

29. Wu Q, Spiryagin M, Cole C (2020) Train energy simulation with locomotive adhesion model. Railw Eng Sci 28(1):75–84

30. Rail Safety and Standards Board (2010) Guidance on testing of wheel slide protection systems fitted on rail vehicles, GM/GN2695, London